corded hologram, and the reconstruction of the entire signal beam is produced. This reconstruction can be brought to focus on a detector array [e.g., charge-coupled devide (CCD) camera]. What makes holographic memories an interesting technology is that changing the angle of the reference by as little as 0.007° during read-out (*27*) will cause the reconstruction to disappear. This makes it possible to superimpose many pages in the same volume (up to 10,000 pages has been demonstrated). Each page can be thought of as an additional layer in a holographic memory disk, leading to storage densities roughly two orders of magnitude better than are possible with DVDs (*28*). Because the recorded pages of data are holograms, it is possible to read them out using phase conjugation (*29*), in which case the hologram is illuminated with a beam that is the same as the reference used during recording except that it propagates backward. This results in the reconstruction of the signal beam that is also propagating backward, and in doing so it comes to focus back at the plane of the SLM. The focused page of data can be directed to a CCD by a beamsplitter (Fig. 6). The advantage of using phase-conjugate readout is that it allows us to be rid of the powerful lens that is required to focus the field of a 10^3 pixel by 10^3 pixel image with good resolution. In the experiment shown in Fig. 5, a page consisting of squares of varying sizes clearly shows that pixels with resolution well below a micrometer are well reconstructed (*30*). Several hundred pages were superimposed in the same crystal shown in Fig. 6. So far, systems like the one in Fig. 5 have not reached commercial success. The main practical success of 3D storage techniques has been the multilayer DVDs with as many as four layers (two-sided, two-layers per side). More ambitious 3D storage systems based on holography or nonlinear optics remain hindered by a lack of suitable materials.

Conclusion

The recent progress in optical information systems may be only the beginning of a long-lasting trend. For instance, optical communications are currently based on intensity detection, and the phase of the transmitted signal is not measured. Coherent communications have advantages of flexibility and signal-to-noise ratio. The emergence of inexpensive laser sources with high coherence and stability will allow their use as local oscillators similar to the way in which local oscillators are used in today's radio communication systems. One of the challenges for the future is the development of efficient methods for optical signals to directly interact with each other in nonlinear media. This is an emerging technology in fiber optics (for instance, semiconductor optical amplifiers used for wavelength conversion), but one that may lead to communication networks composed entirely of optical switching devices.

References and Notes

1. L. Mandel, E. Wolf, *Optical Coherence and Quantum Optics* (Cambridge Univ. Press, New York, 1995).
2. A. Grover, C. P. Lee, A. Yariv, *J. Opt. Soc. Am.* **66**, 306 (1976).
3. J. W. Goodman, *Statistical Optics* (Wiley-Interscience, New York, 1985).
4. D. Gabor, *Nature* **161**, 777 (1948).
5. R. J. Collier, C. B. Burckhardt, L. H. Lin, *Optical Holography* (Academic Press, New York, 1971).
6. Y. N. Denisyuk, *Sov. Phys.-Dokl.* **7**, 543 (1962).
7. ———, *Opt. Spectrosc.* **15**, 279 (1963).
8. D. J. Mark, R. A. Stack, D. J. Brady, D. C. Munson, R. B. Brady, *Science* **284**, 2164 (1999).
9. W. H. Liu, D. Psaltis, G. Barbastathis, *Opt. Lett.* **27**, 854 (2002).
10. S. C. W. Hyde *et al.*, *Opt. Lett.* **20**, 1331 (1995).
11. M. R. Hee *et al.*, *Opt. Lett.* **18**, 950 (1993).
12. M. Ikuta *et al.*, *Appl. Opt.* **41**, 1882 (2002).
13. D. Huang *et al.*, *Science* **254**, 1178 (1991).
14. L. Kazovsky, S. Benedetto, A. Willner, *Optical Fiber Communication Systems* (Artech House, Boston, 1996).
15. B. E. A. Saleh, M. C. Teich, *Fundamentals of Photonics* (Wiley-Interscience, New York, 1991).
16. C. K. Madsen, J. H. Zhao, *Optical Filter Design and Analysis* (Wiley-Interscience, New York, 1999).
17. A. Othonos, *Rev. Sci. Instrum.* **68**, 4309 (1997).
18. G. A Rakuljic, V. Leyva, *Opt. Lett.* **18**, 459 (1993).
19. K. Buse, Hukriede, C. Moser, I. Nee, D. Psaltis, G. Steckman, www.ondax.com/pdf/whitepaper.pdf.
20. J. D. Joannopoulos, R. D. Meade, J. N. Winn, *Photonic Crystals* (Princeton Univ. Press, Princeton, NJ, 1995).
21. J. W. Goodman, F. J. Leonberger, S. Y. Kung, R. A. Athale, *IEEE* **72**, 850 (1984).
22. G. Li *et al.*, *Appl. Opt.-IP* **41**, 348 (2002).
23. S. R. Chinn, E. A. Swanson, *Opt. Lett.* **21**, 899 (1996).
24. D. A. Parthenopoulos, P. M. Rentzepis, *Science* **245**, 843 (1989).
25. M. M. Wang, S. C. Esener, *Appl. Opt.* **39**, 1826 (2000).
26. H. Coufal, D. Psaltis, G. Sincerbox, Eds., *Holographic Data Storage* (Springer-Verlag, New York, 2000).
27. X. An, D. Psaltis, G. W. Burr, *Appl. Opt.* **38**, 386 (1999).
28. G. J. Steckman, A. Pu, D. Psaltis, *Appl. Opt.* **40**, 3387 (2001).
29. E. Chuang, W. Liu, J. Drolet, D. Psaltis, *Proc. IEEE* **87**, 1931 (1999).
30. W. Liu, D. Psaltis, *Opt. Lett.* **24**, 1340 (1999).

31. Special thanks to Z. Liu for critical review of the manuscript and suggestions. I also thank Y. Abu-Mostafa and K. Buse for fruitful discussions, and H.-T. Hsieh for help with the preparation of the manuscript. The work at Caltech is supported by the NSF Center on Neuromorphic Systems Engineering, the Defense Advanced Research Projects Agency (DARPA), and the Air Force Office of Scientific Research (AFOSR).

REVIEW

Coherence with Atoms

Mark A. Kasevich

The past decade has seen dramatic progress in our ability to manipulate and coherently control the motion of atoms. This progress has both fundamental and applied importance. On the one hand, recent experiments are providing new perspectives for the study of quantum phase transitions and highly entangled quantum states. On the other hand, this exquisite control offers the prospect of a new generation of force sensors of unprecedented sensitivity and accuracy.

In 1991, the experimental analog to Young's double-slit experiment using helium atoms was realized (*1*). A beam of helium atoms first illuminated a microfabricated slit that was narrow enough to produce a wavefront capable of coherently illuminating a double-slit structure. A scannable detector recorded the number of atoms arriving at a given position in the far field of the double slit. The expected spatial oscillation in atom counts as the detector was moved across the atom distribution was observed, much as the intensity profile of a beam of light is spatially modulated as it is subjected to a similar series of slits. Nearly coincidentally with this work, three other groups observed atom de Broglie wave interference in interferometer geometries analogous to optical Mach-Zehnder interferometers (*2–4*).

Although it is a fundamental and well-tested tenet of quantum mechanics that wave-like properties are associated with particles, it is remarkable that a collection of particles as complicated as an entire atom can be coaxed to behave in this way. Since these initial experiments, the field of coherent atom optics has grown in many directions (*5*). The past several years have seen explosive growth. This review is meant to provide context for this recent work in terms of past accomplishments and future milestones.

Department of Physics, Stanford University, Stanford, CA 94305–4060, USA.

Deconstructing Decoherence

In the quantum mechanics paradigm, coherence between multiple propagation paths only manifests itself when there is no possibility of observing "which path" the particle follows. However, an interaction with the environment in some sense constitutes an observation of the system and suppresses possible interference. How well isolated does the interfering particle

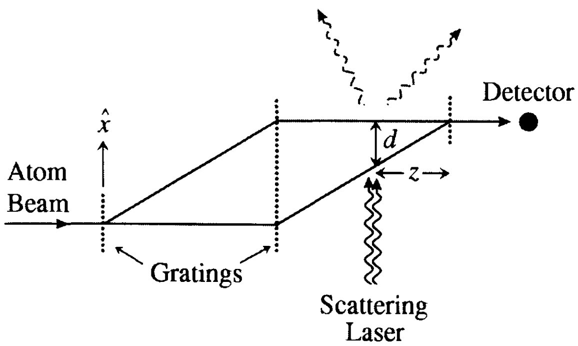

Fig. 1. Schematic of the apparatus used to study wave packet decoherence. Controlled coupling to the environment is realized via resonance fluorescence from a probe laser beam. The strength of the coupling is varied by tuning the intersection distance z, which controls the path separation d; and the laser intensity, which controls the mean number of photons scattering on transit through the laser beam (tuned between 0 and 10). $\hat{x}$, x axis. [Figure courtesy of D. Pritchard, Massachusetts Institute of Technology]

need to be from the environment for coherent effects to manifest themselves? For the systems initially studied, the environment was sufficiently remote, by experimental design, that "which path" information was unavailable.

Recent experiments have explored in a controlled way the effects of bringing the environment much closer (*6*, *7*). For example, a three-grating, Mach-Zehnder-type, de Broglie wave interferometer was used to coherently divide, redirect, and recombine Na de Broglie waves while a variable-intensity resonant probe laser beam provided a controlled coupling to the environment (Fig. 1). This technique enabled a quantitative study to be made of the degree of coherence as a function of the strength of the interaction with the coupling laser. It was observed, for example, that when the laser excitation was done in a way that in principle allowed for the determination of the trajectory of an atom (by imaging, for example, the scattered light), then wavelike interference disappeared. For laser excitation parameters that blurred this determination (for example, low laser intensity or proper choice of the excitation geometry), interference was partially or fully restored. The importance of this work is that it provides for quantitative tests of basic principles, in a regime simple enough for clean comparison with theory but complex enough to explore a rich nontrivial phenomenology. The insights gained from studying benchmark systems provide an experimental foundation for the engineering of more complicated systems, such as those currently under consideration for use in quantum logic devices (*8*).

Bright Matter

The 1997 and 2001 Nobel Prizes recognized the development of two techniques that have allowed for remarkably precise control over atom velocity. In 1997, the first to be recognized was the development of laser cooling methods (*9*); in 2001, the prize was awarded for the observation of Bose-Einstein condensation (BEC) in dilute atomic gases (*10*). Although it was not a prerequisite for studying or exploiting coherent matter-wave effects, the landmark work recognized by these prizes catalyzed experimental progress by providing access to atomic sources of unprecedented brightness and coherence length.

Why is brightness important? Because it directly addresses a technologically challenging, though perhaps conceptually mundane, constraint on the design of an interferometer: The instrument needs to be built so that the observed interference fringe pattern is stationary with respect to all possible particle input conditions. High brightness sources enable substantial particle throughput while maintaining tight control over the input conditions.

Recently, the state of the art for high-flux laser-cooled sources was advanced through the development of a novel Raman sideband cooling technique (*11*). This technique was used to improve the performance of an atom interferometer gravimeter (*12*). Ultimately, this advance could lead to an order of magnitude or more improvement in the performance of these already very sensitive instruments. Although the particle throughputs for these devices still pale in comparison to the number of photons that contribute to interference signals in, for example, fiber-optic gyroscopes ($\sim 10^8$ atoms/s versus $\sim 10^{16}$ photons/s), they are many orders of magnitude higher than those obtained in the first atom interference experiments. Young's double-slit experiment discussed above had count rates of just a few atoms per second.

BEC sources take input state preparation to the logical limit, where nearly all atoms lie in a single quantum state. Thus, all atoms can potentially contribute to the subsequent interference profiles. On the basis of pure signal-to-noise considerations, however, BEC sources suffer from the rather tortuous route required to obtain them (*13*). A truly practical high-flux BEC source still awaits development. From a technological perspective, a goal would be a high-flux continuous-wave BEC source.

This past year saw a substantial step forward toward this development with the realization of the first nearly continuous BEC source (*14*). In this work, a first BEC was replenished through filling from a second BEC, enabling, in principle, continuous and indefinite extraction of condensed atoms from the source. An important aspect of this work was that it demonstrated that the excess energy resulting from the condensate merger was small enough that it could be effectively dissipated through evaporative cooling.

One long-term vision is the integration of a BEC apparatus into compact microelectronic surface assemblies (microtraps). During this past year, several groups have demonstrated the feasibility and practicality of this approach (*15*, *16*). In these experiments, atoms were manipulated by means of the magnetic fields generated by microfabricated wires deposited on surfaces (Fig. 2).

Coherent Waveguides Have Arrived

Our current catalog of atom optics includes microfabricated slits, diffraction gratings, and holographic plates; magnetic waveguides, mirrors, and gratings; and laser light-based waveguides, mirrors, and gratings (*5*).

Which to choose? That is a complicated technical question that involves detailed knowledge of the application and relevant design trade-offs. For example, a laser-based atom diffraction grating has an exceptionally well-known periodicity, because this is determined by the wavelength of the laser. The inherent accuracy of de Broglie wave gyroscopes and accelerometers is tied to the stability of the grating periodicity, so if sensor accuracy is the most important design criterion, then laser-based atom diffraction gratings are a natural choice.

Waveguide-based sensors offer the prospect of small sizes and high sensitivities (but

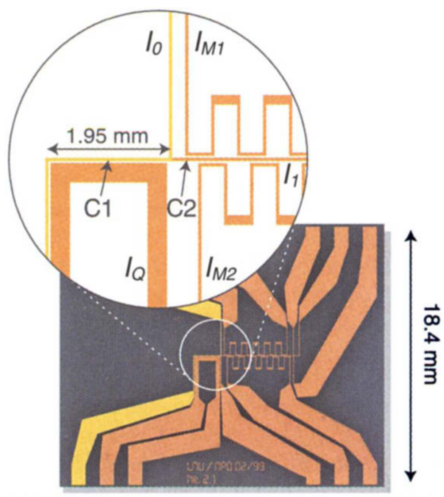

Fig. 2. The microelectronic electrode structure used to create a BEC on a chip. The inset shows the conductor layout used to trap and transport the atoms. C1 and C2 indicate positions of the condensed atoms. I_0, I_{M1}, I_1, I_Q, and I_{M2} are currents used to create the magnetic trapping potential. [Figure courtesy of J. Reichel, Max-Planck-Institut für Quantenoptik]

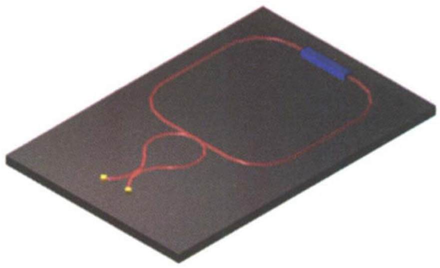

Fig. 3. Schematic of a possible geometry for a waveguide Sagnac-effect atom gyroscope. An atom gain element (blue) feeds a loop waveguide structure (red). Atoms are extracted and detected using correlated-state techniques to achieve sub-shot-noise limited detection (yellow). The past year has seen substantial progress in the development of each relevant element. A loop 10 cm by 10 cm might achieve a 10^6-fold improvement in sensitivity to rotations for intermediate acquisition bandwidths (tens of seconds), and a 10^4-fold improvement for high frequencies (less than 1 s). The long-term stability and accuracy are difficult to project.

questionable accuracies). In these devices, small wires, deposited on a substrate, are used to create magnetic field gradients strong enough to guide atoms along paths defined by the wires, much as photons are guided by optical fiber. The past year has seen the first realization of coherent guided-wave devices (*17*, *18*). Although it is still too early to speculate on their full impact, a promising sensor application is rotation sensing, based on operating principles similar to those of fiber-optic gyroscopes (Fig. 3).

The first coherent transport demonstrations have identified substantial technical hurdles before practical devices might be realized. Minor imperfections in the geometry of the guides have been shown to lead to rather substantial deviations from ideal particle transport through the guide. Pictures of atoms released from the guides reveal kinks and blockages that have their origin in manufacturing asymmetries or coupling to the surface. Future work is needed to identify mitigation strategies.

Next-Generation Sensors

The steady evolution in the sophistication of atom interferometric methods is now at the point where laboratory sensors based on atom interferometric techniques compete favorably in key performance criteria with other state-of-the-art sensors. For example, rotations (*19*) and accelerations (*20*) can be monitored with extremely high accuracy and sensitivity through careful measurement of the de Broglie wave propagation phase shifts in Mach-Zehnder configurations. The ultimate utility of a sensor depends on many factors beyond laboratory performance benchmarks. Atom interferometric sensors have matured to the point where their utility can be evaluated in terms of criteria such as cost, durability, weight, and so so. Extrapolations based on laboratory sensors are promising. Applications that lie in the near future include the development of instruments to detect gravitational gradients from moving platforms (*21*) and gravity-compensated navigation systems (*22*). Fig. 4 illustrates a laboratory gravity-gradient sensor (*23*), which has been used to measure the gravitational influence of a well-characterized Pb source mass on interference signals.

Beyond Single-Particle Interference

Access to BEC sources has brought much more than brightness to atom optics. It has sharpened our conceptual understanding of many-body systems and perhaps may enable a new family of interferometry techniques. As an example, consider the following paradigm experiment: First, produce two spatially separated independent condensates of identical atoms. Then release the atoms from their confining potentials in such a way that the two resulting clouds of atoms overlap. Finally, record the resulting atom density distribution. Will interference be observed or not?

On first analysis, the answer seems trivial. If an individual condensate is described by a macroscopic wave function $\Psi = \sqrt{n}\, e^{i\,\phi}$, where n is the particle density distribution and ϕ is an overall macroscopic phase, then two such entities ought to interfere just as two electromagnetic waves interfere. The interference pattern will be determined by the relative phase between the two condensates and the details of atom propagation between the sources and the detection volumes.

But what sets the relative phase? Even more troubling, how can a phase exist at all? The quantum mechanics of an ensemble of indistinguishable bosons (such as photons or atoms in a BEC) requires complementarity between the fluctuations in the number of particles in the ensemble ΔN and the fluctuations in phase $\Delta\phi$ associated with the field. In this example, it is possible that each condensate contains a fixed and known number of particles. This implies complete uncertainty in the phase of each ensemble. If the phase of each condensate is completely uncertain, how can they interfere? This experiment was carried out in 1997 (*24*); the result is shown in Fig. 5. The two condensates interfered!

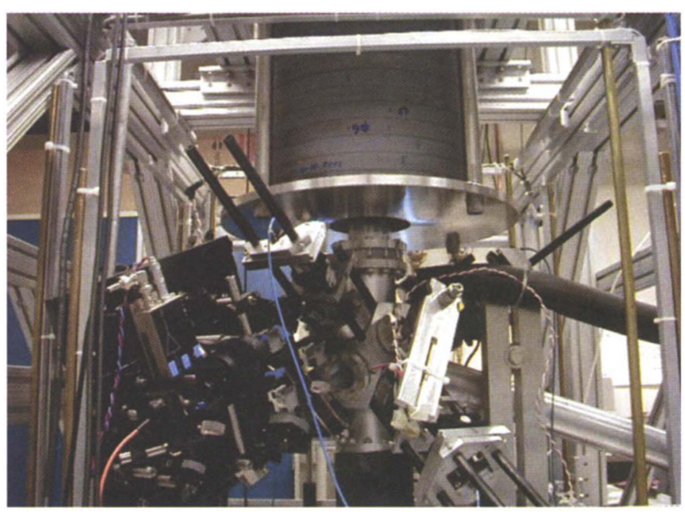

Fig. 4. Laboratory gravity gradiometer at Yale University, used to measure the gravitational influence of a well-characterized Pb test mass on a spatially separated pair of atom interferometer accelerometers.

Despite its superficial similarity to Young's double-slit experiment described above, the situation described in this two-condensate interference problem is very different. In the two-slit problem, the relative phase between the interfering beams is established by the geometry of the slits and the fact that the slits are illuminated from a single coherent wavefront. In this experiment, we are left to wonder what sets the relative phase.

To gain insight into this question, it is useful to analyze a simpler problem first. Rather than two condensates, consider just two identical bosons, initially localized at positions $\mathbf{x}_a$ and $\mathbf{x}_b$. By considering the symmetrized wave function for two freely evolving wave packets, it can be shown that the probability P of detecting one particle at position $\mathbf{x}_1$ and another at $\mathbf{x}_2$ is $P \sim \cos^2\delta\phi$, with $\delta\phi \sim (\mathbf{x}_1 - \mathbf{x}_2) \times (\mathbf{x}_a - \mathbf{x}_b)$. The important point is that the probability of the second detection depends on what was observed in the first detection (in this case, it varies sinusoidally), whereas the probability of detecting an individual particle is uniform. [An interesting consequence is that the probability of detecting the two particles at nearly the same position $\mathbf{x}_1 \sim \mathbf{x}_2$ is twice the probability averaged over all positions (the Hanbury-Brown-Twiss effect for optical sources). This effect was observed in 1996 with laser-cooled bosonic Ne atoms (*25*). Measurements of the energy associated with binary collisions (*26*) and three-body loss rates in condensed atomic clouds (*27*) are also sensitive probes for this and related effects.]

Now let's return to the problem of two interfering condensates, each with a definite number of atoms. The basic idea is that the detection of one atom influences the probability distributions for the detection of subsequent atoms, in such a way that the spatial distribution of atoms collapses to the fringe

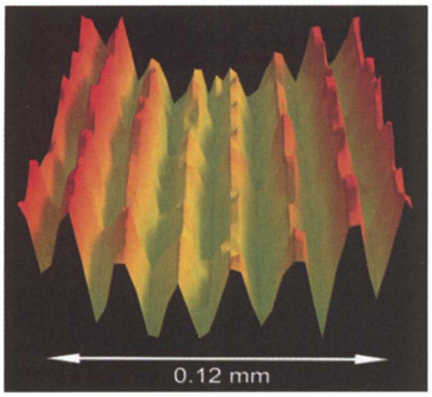

Fig. 5. Interference fringes resulting from the overlap of atoms released from two independent BEC sources. [Figure courtesy of W. Ketterle, Massachusetts Institute of Technology]

pattern observed in the interference experiments. It has been shown, both analytically (*28*) and through numerical simulation (*29*), that the overall position of the fringe—the phase associated with the interference—depends on the detailed way in which the individual atom detections occur. Remarkably, the process of detection can be thought of as selecting a phase for the interference. An experimental consequence is that the phase of the interference pattern jumps from shot to shot. Thus, the phase is uncertain until the time of measurement for this idealized model. In the experiments of (*24*), the phase of the observed interference pattern did fluctuate, though it was not possible to unambiguously identify the mechanism of the fluctuations, because technical noise sources were also present in the measurements.

The interference properties of a two-mode system with a definite number of particles in each mode can be manipulated in a surprising way that may have important implications for future atom interferometric sensors. Consider the case where the two condensates are mixed on a beam splitter (in practice, this beam splitter could be realized by suddenly coupling the two condensates using a tunneling process). If the relative phase is uncertain before measurement, then after the beam splitter the many-particle wave function for each ensemble should have number fluctuations on the order of the initial number of atoms. By the number/phase uncertainly relation, we expect the phase (or, more precisely, the relative phase between the two output ports of the beam splitter) to be defined at a level $\Delta\phi \sim 1/N$. In contrast, the phase uncertainty associated with a classical field (coherent state) scales as $1/\sqrt{N}$. Because the phase uncertainty ultimately sets the limits to which small phase shifts can be resolved, a factor of $\sqrt{N}$ enhancement in interferometer precision might be realized. One proposed implementation involves the use of two sequential beam splitters in the Mach-Zehnder topology (*30*, *31*).

What's the catch? First, the initial number of atoms in at least one of the modes needs to be known, and second, atoms need to be counted at one of the output ports with single-atom resolution. Technical realization of these conditions is currently an active area of pursuit for many research groups. For example, cavity quantum electrodynamics techniques might be used both to measure the initial number of atoms in a mode and to count atoms at the single-atom level [see the review article by Mabuchi in this issue (*32*)] (*33*). Recently, the use of high-gain four-wave mixing processes has been demonstrated to generate correlated beams with precisely balanced numbers of particles in each beam (*34*). Insulating/squeezed states in optical lattice potentials, described below, may also enable realization of these types of schemes. Finally, the internal degrees of freedom of an ensemble of atoms or ions can, under certain observation conditions, be manipulated to achieve similar sensitivity enhancements (*35–37*).

The ultimate efficacy of these methods hinges on the development and refinement of experimental methods to prepare and detect exotic many-atom quantum states. At stake is a factor of 1000 times or more in sensitivity for atom optics sensors.

Classical Josephson Effects

By introducing a strong enough coupling between the two condensed sources (with a tunnel junction), it is possible to prepare the system in a state of well-defined relative phase. In this case, the analogy with the condensate initial Young's configuration is much stronger. Here, the ground state of the system is one in which every particle is itself in a linear superposition of the two condensate positions. As a consequence, the number of atoms in a given trap is uncertain, even though the total number of atoms can be fixed. For large numbers of atoms, the atom number distribution becomes close to that of a coherent state, which can be seen from a binomial expansion of the superposition state wave function.

Interference in this regime has been observed in optical lattice experiments (*38*, *39*), where a single condensate is transferred into a corrugated potential defined by a laser standing wave. The potential is deep enough that the condensate segregates into an array of trapped atoms, but shallow enough that atoms can tunnel from trap to trap in a suitably short time. When atoms are suddenly released from the lattice, they expand and interfere in a way analogous to the interference of single particles through a multiple-slit mask. For the experiments, atomic densities were kept low enough that nonlinear effects (discussed below) could be safely ignored.

The dynamic response of the tunnel array system to external forces has close analogies with Josephson effects in superconducting systems (*40*). For example, when a potential energy gradient is applied across the array, the system oscillates at a frequency analogous to the alternating current (ac) Josephson frequency. Interference in this regime has been used to measure the acceleration due to gravity by monitoring the time evolution of the interference pattern due to the presence of the external gravitational potential (Fig. 6) (*38*, *41*). More recent studies have used atom transport observations to directly measure the critical current (*39*).

Exploiting Nonlinearities

In optical systems, intensity-dependent index of refraction nonlinearities are used to generate squeezed optical states. In BEC atomic systems, binary atom-atom collisions lead to an analogous nonlinearity for de Broglie waves. This mean-field nonlinearity has recently enabled, for example, observation of four-wave mixing (*42*) and soliton formation (*43*, *44*). The nonlinearity also offers a new and powerful handle for the manipulation and creation of nontrivial many-atom states and dramatically influences the coherence properties of atomic systems (*45*).

A recent experiment beautifully illustrates

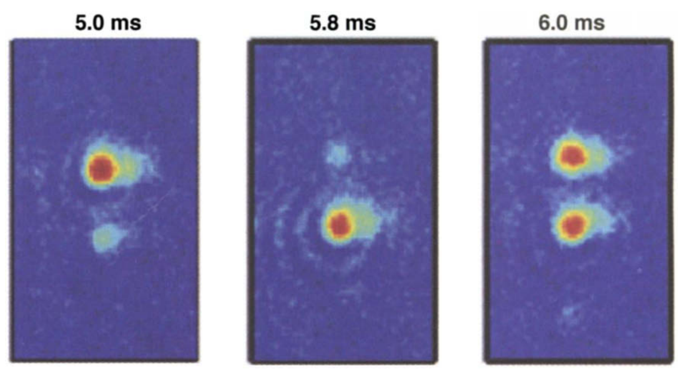

Fig. 6. AC Josephson effect in optical lattices, as observed through the interference profile of atoms suddenly released from a vertically oriented, one-dimensional optical lattice. The relative phase ϕ between adjacent wells evolves according to the Josephson relation $(h/2\pi)d\phi/dt = V$, where h is Planck's constant, t is time, and V is the chemical potential difference between adjacent wells. This evolution results in an oscillation of the populations of diffraction lobes in the interference signals. In this work, V is determined by gravity. The time label references the time interval that the atoms were held in the combined gravitational plus optical lattice potential before being released and imaged.

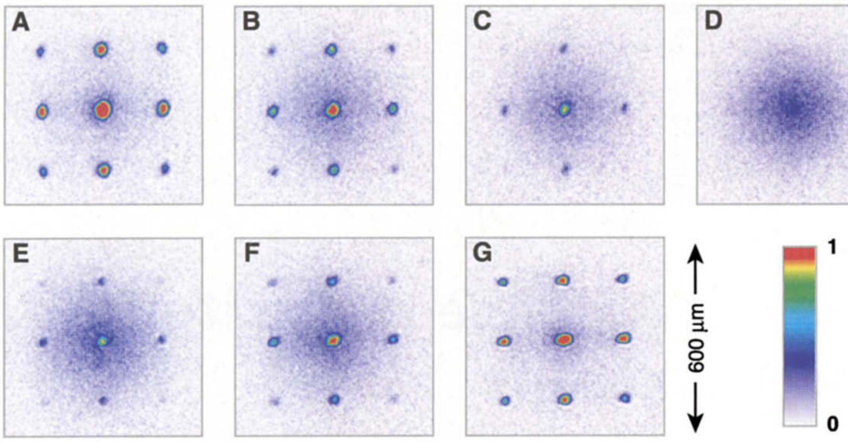

Fig. 7. Quantum state collapse and revival, as observed in the interference profiles of atoms released from a three-dimensional optical lattice. The images (**A** to **G**) show the time evolution of the interference pattern for lattice hold times ranging from 0 to 550 μs. The sharp diffraction peaks observed in (A) and (G) indicate the initial and revived phase coherence between adjacent lattice sites. [Figure courtesy of I. Bloch, Max-Planck-Institut für Quantenoptik]

the influence of this nonlinearity on the evolution of a coherent many-atom state (*46*). In this work, a BEC was loaded into a three-dimensional optical lattice. Initially, the corrugated potential was shallow enough that tunnelling established phase coherence across the array. As a consequence, the atom number distribution in each lattice site followed a Poissonian distribution. The lattice depth was then suddenly raised to a level that suppressed transport between adjacent wells, essentially freezing a Poissonian atom number distribution into each site. In the absence of a nonlinear interaction, the coherence across the array is maintained as time evolves. However, a nonlinearity changes the energy associated with each component number state in the Poissonian distribution, leading to a nonstationary evolution of the quantum state at each site. The subsequent observation was a periodic collapse and revival of the resulting interference contrast after atoms were released from the array, as a function of the hold time in the lattice, indicative of the relative phases of the component number states dephasing then rephasing with respect to one another (Fig. 7).

Lattice systems have also been used to prepare other nontrivial many-body states by controlling the relative strength of the tunneling rate and the strength of the mean-field nonlinearity. As the tunneling rate is decreased (by increasing the depth of the lattice), it becomes energetically unfavorable to support onsite number fluctuations, and the number variance at each site drops below the initial Poissonian level. By analogy with quantum optical systems, the many-body state at each site becomes number-squeezed. When the number variance drops below $\sim$1 atom on each site, the system undergoes an insulating phase transition to a state characterized by a fixed number of atoms per lattice site (for commensurate fillings and translationally invariant lattices).

Experimentally, these effects have been explored by loading a BEC into a corrugated optical lattice potential, and then adiabatically manipulating the strength of the potential (*47*, *48*). The relative phase coherence between adjacent sites was probed interferometrically by suddenly releasing atoms from the confining lattice. For well-defined relative phases between adjacent sites, interference leads to the emergence of sharp diffraction peaks. However, as the number variance decreases (and phase variance correspondingly increases), these sharp lobes are suppressed and are replaced by a diffuse incoherent background. The suppression of sharp interference peaks is a consequence of the fact that many lattice sites contribute to the interference pattern. In this case, the detection process can be thought to select an ensemble of random phases. The work in (*48*) provided clear evidence of a transition point where long-range phase coherence rather suddenly disappeared. This transition point occurs for conditions consistent with those expected from theoretical estimates for a Mott-insulator quantum phase transition (*49*, *50*).

Concluding Remarks and Outlook

These experiments raise many questions. How does the many-body state of the array evolve when the lattice conditions are suddenly quenched from conditions associated with an insulating state to one associated with long-range phase coherence? What happens at finite temperature, especially near the transition point? Unlike the first atom interference demonstrations, where the quantum system (a single atom) was well isolated from the environment, here the environment (a finite temperature reservoir in thermal contact with the quantum state) is unnervingly close to a possibly fragile, many-atom quantum system. And unlike the recent decoherence studies discussed at the beginning of this review, exact theory is unavailable. The qualitative issues are very similar to those of quantum information science (*8*): The size of the Hilbert space is exponentially large, the role of decoherence needs clarification, and the need for further experimental and theoretical work is compelling.

References and Notes

1. O. Carnal, J. Mlynek, *Phys. Rev. Lett.* **66**, 2689 (1991).
2. F. Riehle, T. Kisters, A. Witte, J. Helmcke, C. J. Bordé, *Phys. Rev. Lett.* **67**, 177 (1991).
3. M. Kasevich, S. Chu, *Phys. Rev. Lett.* **67**, 181 (1991).
4. D. W. Keith, C. R. Ekstrom, Q. A. Turchette, D. E. Pritchard, *Phys. Rev. Lett.* **66**, 2693 (1991).
5. P. Berman, Ed., *Atom Interferometry* (Academic Press, New York, 1997).
6. D. A. Kokorowski, A. D. Cronin, T. D. Roberts, D. E. Pritchard, *Phys. Rev. Lett.* **86**, 2191 (2001).
7. M. S. Chapman *et al.*, *Phys. Rev. Lett.* **75**, 3783 (1995).
8. M. Nielsen, I. Chuang, *Quantum Computation and Quantum Information* (Cambridge Univ. Press, New York, 2000).
9. W. Phillips, C. Cohen-Tannoudji, *Phys. Today*, **43**, 33 (1990).
10. E. Cornell, C. Wieman, *Sci. Am.* **278**, 40 (1998).
11. A. J. Kerman, V. Vuletic, C. Chin, S. Chu, *Phys. Rev. Lett.* **84**, 439 (2000).
12. P. Treutlein, K. Y. Chung, S. Chu, *Phys. Rev. A* **63**, 051401 (2001).
13. W. Ketterle, N. J. VanDruten, *Adv. At. Mol. Opt. Phys.* **37**, 181 (1996).
14. A. P. Chikkatur *et al.*, *Science* **296**, 2193 (2002).
15. W. Hänsel, P. Hommelhoff, T. W. Hänsch, J. Reichel, *Nature* **413**, 498 (2001).
16. H. Ott, J. Fortagh, G. Schlotterbeck, A. Grossmann, C. Zimmermann, *Phys. Rev. Lett.* **87**, 230401 (2001).
17. A. E. Leanhardt *et al.*, *Phys. Rev. Lett.* **89**, 040401 (2002).
18. J. Fortagh, H. Ott, S. Kraft, C. Zimmermann, preprint available at http://xxx.lanl/gov/abs/cond-mat/0205310v2 (2002).
19. T. L. Gustavson, A. Landragin, M. A. Kasevich, *Classical Quantum Grav.* **17**, 2385 (2000).
20. A. Peters, C. Keng Yeow, S. Chu, *Nature* **400**, 849 (1999).
21. E. Leeuwen, *Leading Edge* **19**, 1296 (2000).
22. A. H. Zorn, in *Proceedings of the IEEE Position, Location and Navigation Symposium*, Palm Springs, CA, 15 to 18 April 2002 (IEEE, Piscataway, NJ, 2002), pp. 66–73.
23. J. M. McGuirk, G. T. Foster, J. B. Fixler, M. J. Snadden, M. A. Kasevich, *Phys. Rev. A* **65**, 033608 (2002).
24. M. R. Andrews *et al.*, *Science* **275**, 637 (1997).
25. M. Yasuda, F. Shimizu, *Phys. Rev. Lett.* **77**, 3090 (1996).
26. W. Ketterle, H. J. Miesner, *Phys. Rev. A* **56**, 3291 (1997).
27. E. A. Bert *et al.*, *Phys. Rev. Lett.* **79**, 337 (1997).
28. Y. Castin, J. Dalibard, *Phys. Rev. A* **55**, 4330 (1997).
29. J. Javanainen, S. M. Yoo, *Phys. Rev. Lett.* **76**, 161 (1996).
30. M. Holland, K. Burnett, *Phys. Rev. Lett.* **71**, 1355 (1993).
31. P. Bouyer, M. A. Kasevich, *Phys. Rev. A* **56**, R1083 (1997).
32. H. Mabuchi, A. C. Doherty, *Science* **298**, 1372 (2002).
33. ———, Q. A. Turchette, M. S. Chapman, H. J. Kimble, *Opt. Lett.* **21**, 1393 (1996).
34. J. M. Vogels, K. Xu, W. Ketterle, *Phys. Rev. Lett.* **89**, 020401 (2002).
35. M. Kitagawa, M. Ueda, *Phys. Rev. A* **47**, 5138 (1993).
36. D. J. Wineland, J. J. Bollinger, W. M. Itano, F. L. Moore, D. J. Heinzen, *Phys. Rev. A* **46**, R6797 (1992).
37. A. Kuzmich, L. Mandel, N. P. Bigelow, *Phys. Rev. Lett.* **85**, 1594 (2000).

38. B. Anderson, M. A. Kasevich, in *Proceedings of the International School of Physics "Enrico Fermi,"* M. Inguscio, S. Stringari, C. E. Wieman, Eds. (IOS Press, Amsterdam, 1999).
39. F. S. Cataliotti *et al.*, *Science* **293**, 843 (2001).
40. A. Barone, G. Paterno, *Physics and Applications of the Josephson Effect* (Wiley, New York, 1982).
41. B. P. Anderson, M. A. Kasevich, *Science* **282**, 1686 (1998).
42. L. Deng *et al.*, *Nature* **398**, 218 (1999).
43. S. Burger *et al.*, *Phys. Rev. Lett.* **83**, 5198 (1999).
44. J. Denschlag *et al.*, *Science* **287**, 97 (2000).
45. A. Sorensen, L. M. Duan, J. I. Cirac, P. Zoller, *Nature* **409**, 63 (2001).
46. M. Greiner, T. W. Hänsch, I. Bloch, *Nature* **419**, 51 (2002).
47. C. Orzel, A. K. Tuchman, M. L. Fenselau, M. Yasuda, M. A. Kasevich, *Science* **291**, 2386 (2001).
48. M. Greiner, O. Mandel, T. Esslinger, T. Hänsch, I. Bloch, *Nature* **415**, 39 (2002).
49. D. Jaksch, C. Bruder, J. I. Cirac, C. W. Gardiner, P. Zoller, *Phys. Rev. Lett.* **81**, 3108 (1998).
50. S. Sachdev, *Quantum Phase Transitions* (Cambridge Univ. Press, New York, 1999).
51. Our work is supported by NSF, the Office of Naval Research, the Army Research Office, NASA, and the Air Force Research Laboratory.

REVIEW

Spontaneous Bose Coherence of Excitons and Polaritons

David Snoke

In the past decade, there has been an increasing number of experiments on spontaneous Bose coherence of excitons and polaritons. Four major areas of research are reviewed here: three-dimensional excitons in the bulk semiconductor Cu_2O, two-dimensional excitons in coupled quantum wells, Coulomb drag experiments in coupled two-dimensional electron gases, and polaritons in semiconductor microcavities. The unifying theory of all these experiments is the effect of spontaneous symmetry breaking in the Bose-Einstein condensation phase transition.

Numerous recent experiments have studied coherence in semiconductor systems. In most of these experiments, the coherence is generated from a coherent laser that excites the system. The laser itself acquires coherence because a selected optical state is amplified. In the past two decades, however, several experimenters have pursued the possibility of spontaneous coherence in semiconductor systems. In such a case, no single state is selected for amplification. Instead, coherence appears in a state selected by the system itself by means of a thermodynamic phase transition.

The phase transition that can cause this is Bose-Einstein condensation (BEC) of excitons or polaritons. In this phase transition, a macroscopic number of particles enter a single quantum state, forming a coherent state with definite phase by the process known as "spontaneous symmetry breaking" (*1*). The underlying physics is the same as BEC of atoms, seen in superfluid helium or, more recently, in alkali atoms in magneto-optical traps (*2*, *3*) and in spin-polarized hydrogen (*4*). Excitons and polaritons, quanta of excitation that are integer-spin bosons, often have an effective mass and a long lifetime, so that they can be treated theoretically as metastable atom-like particles. As such, the laws of thermodynamics apply and BEC is expected at a low temperature, typically a few kelvin. After initial proposals in the 1960s (*5*, *6*), the theoretical basis for Bose condensation of excitons was laid down in a number of papers (*7–10*) in the 1970s and 1980s and has continued to attract theoretical interest (*11–13*).

Department of Physics, University of Pittsburgh, 3941 O'Hara Street, Pittsburgh, PA 15260, USA.

Phase Transitions of Excitons

As excitations of the medium, excitons and polaritons are not strictly distinguishable from photon states. Figure 1 shows a typical dispersion relation in a bulk semiconductor. At energy well below the band gap, the excitations are photon-like and have the dispersion relation

$$\hbar\omega = \hbar\left(\frac{c}{n}\right) k \qquad (1)$$

where $\hbar$ is Planck's constant divided by 2π, ω is the photon frequency, c is the speed of light, n is the index of refraction of the medium, and k is the photon wave number. In the opposite limit, at high energy and momentum, one can view the fundamental excitation of the medium as taking an electron

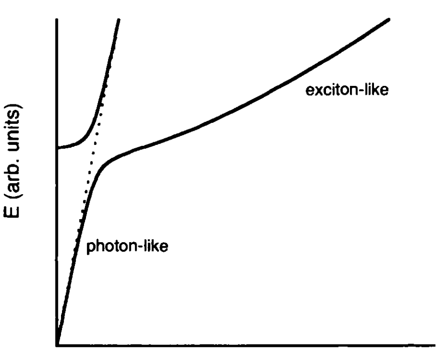

Fig. 1. A typical polariton dispersion relation in a semiconductor. The exciton energy *E*, alone, is given by Eq. 2. At low momentum, the exciton state mixes with the photon states in the medium. These mixed states are called polaritons. The dashed line gives the photon dispersion without mixing.

from the valence band to the conduction band, leaving behind a hole (an empty state) in the valence band. In typical semiconductors, both the electron in the conduction band and the hole in the valence band move freely, with an effective mass on the order of the free electron mass in a vacuum. The Coulomb attraction between the negative electron and the positive hole leads to the bound states known as Wannier excitons. The energy of the excitations in this limit is simply given by the band gap energy (E_{gap}) minus the Rydberg binding energy of the excitons, calculated using the hydrogenic Rydberg formula, plus the kinetic energy of the pair

$$\hbar\omega = E_{gap} - \frac{e^4 m_r}{2\epsilon^2\hbar^2} + \frac{\hbar^2 k^2}{2m_{tot}} \qquad (2)$$

where e is the electron charge, ε is the dielectric constant of the medium, m_r is the reduced mass, and m_{tot} is the total effective mass of the electron and hole. When the photon energy is comparable to the exciton energy, the curves given by Eq. 1 and Eq. 2 cross, and mixing of the states occurs (Fig. 1). The excitations in the region of the mixing are known as polaritons. As seen in Fig. 1, the photon states merge continuously into the polariton states, which merge continuously into the exciton states. All three of these states are bosonic states; that is, they obey the law of stimulated emission derived from the properties of the bosonic quantum field operators.

Some researchers over the years have preferred to say that excitons and polaritons are only approximately bosons, because at high density the Fermi statistics of the underlying electrons and holes become important. Of course, atoms such as helium and hydrogen are only approximately bosons in this sense, also, as they are constructed from fermions, and the Pauli exclusion from these component particles becomes significant at high density. The relevant issue, however, is whether the interactions between the particles are strong enough to destroy the pair corre-